This Page Is Inserted by IFW Operations
and is not a part of the Official Record

BEST AVAILABLE IMAGES

Defective images within this document are accurate representations of the original documents submitted by the applicant.

Defects in the images may include (but are not limited to):

- BLACK BORDERS
- TEXT CUT OFF AT TOP, BOTTOM OR SIDES
- FADED TEXT
- ILLEGIBLE TEXT
- SKEWED/SLANTED IMAGES
- COLORED PHOTOS
- BLACK OR VERY BLACK AND WHITE DARK PHOTOS
- GRAY SCALE DOCUMENTS

IMAGES ARE BEST AVAILABLE COPY.

As rescanning documents *will not* correct images,
Please do not report the images to the
Image Problem Mailbox.

RECEIVED
JUL 22 2004
TC 1700

OIPE JC34
JUL 19 2004
PATENT & TRADEMARK OFFICE

IN THE UNITED STATES PATENT AND TRADEMARK OFFICE

Application Number	:	09/334,986	Confirmation No. 5950
Applicants	:	WARD, Andrew Mark; et al	
Filed	:	June 17, 1999	
Tech Cntr/AU	:	1754	
Examiner	:	Wayne A. Langel	
Entitled	:	Process for Oxidation of Ammonia	
Attorney Reference	:	083255-0303611	
Customer Number	:	00909	

Commissioner for Patents
P.O. Box 1450
Alexandria, Virginia 22313-1450

DECLARATION UNDER 37 C.F.R. §1.132

Sir:

I, Sean Alexander Axon, of 8 Ettersgill Close, Eaglescliffe, United Kingdom, declare:

1. I am of British nationality and earned a BSc degree in chemistry from the University of Liverpool John Moores and a PhD from the University of Cambridge, England in 1988 and 1991, respectively. I have since been working in the field of catalysis, primarily heterogeneous catalysis.

2. In 1999, I joined the Research Department of the Synetix business of *ICI Chemical & Polymers, Ltd.,* a subsidiary of *Imperial Chemical Industries, PLC.* Following the purchase of the Synetix business by Johnson Matthey PLC in 2002, I am now employed by *Johnson Matthey PLC* in the Process Catalysts and Technologies section

of Johnson Matthey Catalysts Division, as the Manufacturing Science Manager for the Johnson Matthey Catalyst business - responsible for strategic research in homogeneous and heterogeneous catalysis.

3. I am a member of Royal Society of Chemistry's solid-state committee and am an active participant in of EPSRC perovskite network. From October 1999 to date I have been responsible for the development of perovskite catalysts for ammonia oxidation.

4. I have read and understood the objections raised by the Examiner in the Office Action mailed April 20th 2004.

5. Following the procedure set forth in Example 2 of the present application, I conducted or had conducted on my behalf the following experiment:

   Catalysts having the composition $La_{0.98}Sr_{0.02}CoO_3$ and $La_{0.98}Ce_{0.02}CoO_3$ were prepared with final calcination at 900°C for 6 hours. The catalysts were then tested for their efficiency (i.e. the percentage of the ammonia converted to NO and NO_2) in a lab-scale ammonia oxidation reactor. The catalysts were tested twice under the same conditions.

   About 60 g of a pelleted catalyst was placed, as a 50 mm bed supported on a stainless steel gauze, in a stainless steel tubular reactor of 28 mm i.d. A mixture of ammonia (10-10.5% by volume) and air was preheated to about 180°C and passed though the reactor. The air was fed at 2 m^3/hour. The exothermic oxidation reaction taking place on the catalyst raised the gas temperatures to 850-900°C. The resulting product gas

RECEIVED
JUL 22 2004
TC 1700

mixture was analysed by mass spectroscopy and the efficiency calculated by taking the average ammonia conversion to NO/NO_2 over a two hour period, measured after steady state conditions had been established. The reaction was stopped by switching off the ammonia and cooling the catalyst under air. The process was then repeated. A small improvement in efficiency is normally observed for the second run due to catalyst conditioning. The results were as follows;

Catalyst	Run	Efficiency	Average
$La_{0.98}Ce_{0.02}CoO_3$	1	88.4	90.7
	2	93.0	
$La_{0.98}Sr_{0.02}CoO_3$	1	87.1	88.1
	2	89.1	

6. It is my belief that the higher efficiency figures for the first, second and average values for the Ce-doped $LaCeCoO_3$ catalyst compared to the Sr-doped $LaSrCoO_3$ catalyst are not suggested by and would not have been obvious from the disclosure of Quinlan. In particular, Quinlan does not suggest that different catalytic behavior might arise by including variable valence elements cerium and praseodymium in the perovskite structure. The increase in efficiency demonstrated is significant, for example, in terms of nitric oxide production due to the scale of industrial operations.

7. It is my belief that inclusion of a variable-valency cation selected from cerium and praseodymium in the A-site of the cobalt perovskite catalyst leads to improved catalytic performance because of their ability to 'shuttle' between the +4 and +3 oxidation states. Divalent strontium does not have this ability. However, it is known that inclusion of cerium and praseodymium in the perovskite structure is difficult whereas inclusion of strontium is relatively straightforward. In this regard, the 'solubility' of strontium in a lanthanum cobaltate perovskite is high. In contrast, it is known that the 'solubility' of cerium in the lanthanum perovskite structure is low and

that its inclusion is more difficult. This difference in behavior is discussed in a paper co-authored by myself that published in 2002 (*Chem. Comm.*, 2706, 2002).

8. In view of the similar redox behavior of cerium and praseodymium (see, e.g., *"A New Concise Inorganic Chemistry"*, 3rd Edition, by J. D. Lee, pages 394-396, 1982), it is my opinion that similar results as shown for the cerium-doped catalyst would be achieved for a praseodymium-doped catalyst.

9. It is my further belief that a skilled person with a knowledge of the low solubility of cerium would not have been motivated by the disclosure of Quinlan to prepare catalysts of the present invention with an expectation of success.

10. It is also my belief that the non-variable-valency cation may be selected from yttrium and the non-variable valency rare earth elements such as lanthanum or neodymium because such elements are known to form stable perovskite structures. In particular, it is known that these elements may all provide suitable A-site elements in a perovskite structure (see for example, *"Structure and Reactivity of Perovskite-Type Oxides"* by Tejuca et al, 1989, pages 240-241).

11. I further declare that all statements made herein of my own knowledge are true and that all statements made on information and belief are believed to be true; and further that these statements were made with the knowledge that willful false statements and the like so made are punishable by fine or imprisonment, or both, under Section 1001 of Title 18 of the United States Code and that such willful false statements may jeopardize the validity of the application or any patent issuing thereon.

Signed and declared at Billingham, England, this 7th day of July, 2004.

Sean A.

Sean Alexander Axon

COMMUNICATION

ChemComm www.rsc.org/chemcomm

Solubility of cerium in $LaCoO_3$–influence on catalytic activity

S. A. French,*[a] C. R. A. Catlow,[a] R. J. Oldman,[a] S. C. Rogers[b] and S. A. Axon[c]

[a] *The Royal Institution of Great Britain, 21 Albemarle St, London, UK W1S 4BS. E-mail: sam@ri.ac.uk*

[b] *ICI Strategic Technology Group, Wilton Centre, PO Box 90, Redcar, UK TS90 8JE*

[c] *Synetix, Belasis Avenue, Billingham, UK TS23 1LB*

Received (in Cambridge, UK) 28th August 2002, Accepted 20th September 2002
First published as an Advance Article on the web 18th October 2002

The recent interest in the catalytic properties of lanthanum perovskites for methane combustion and three way catalysis has led to considerable debate as to their structure and defect chemistry. We have investigated the doping of $LaCoO_3$ with the tetravalent cerium cation using atomistic simulation techniques. We have compared three routes for cerium insertion and identified the favoured doping mechanism, which explain experimental observations relating to the effect of cerium on catalytic activity.

Lanthanum perovskite materials have been investigated for many applications, such as fuel cells, hydrocarbon combustion, exhaust depollution and catalytic membranes. Of particular interest to us are new high temperature oxidation catalysts capitalising on the outstanding structural and thermal stability of perovskites under aggressive reaction conditions. The mechanisms of oxidation at the catalytic active sites in the lanthanum perovskites are, however, still open to considerable debate. Dependent upon the synthesis conditions, the catalyst pre-treatment and the operating conditions, the material exhibits different behaviour, while the inclusion of dopants in the perovskite lattice adds further complexity. However, it has become clear that two types of oxygen play a vital rôle in the catalysis. *Suprafacial* oxygen has been identified as surface adsorbed oxygen in equilibrium with gas phase oxygen and is the dominant reactant species at low temperature, while at higher temperature (typically >550 °C) due to the high ionic conductivity of these materials, *intrafacial* lattice oxygen becomes available for catalysis and an ion-redox catalysed reaction becomes possible.[1–3] Within this descriptive framework, a number of catalytic oxidation regimes can exist as a function of temperature depending on the identity of the perovskite B site transition metal, the inclusion of dopants, particularly at the La site and the specific reaction under consideration.

Of particular interest is $LaCoO_3$ where catalytic behaviour can be mediated by both divalent ion (*e.g.* Sr^{2+}) doping at the La site and tetravalent ion (Ce^{4+}) doping. While the effect of Sr^{2+} doping is relatively well understood experimentally and theoretically in terms of formation of compensating oxygen ion lattice vacancies,[4] the interpretation of the effect of Ce^{4+} doping is complicated by formation of mixed phase materials with segregation of CeO_2. For example, doping with low levels of Ce ($x \sim 0.05$ in $La_{1-x}Ce_xCoO_3$) appears to lead to a small drop in catalytic activity for the lower temperature regime until at higher cerium levels, when CeO_2 is readily detected by XRD, activity returns.[5,6] However, recent work on CH_4 combustion indicates that phase segregated CeO_2 would have relatively low activity compared to $LaCoO_3$. Enhancement in activity at high temperature is therefore dominated by the Ce dopant acting within the $LaCoO_3$ surface lattice.[7]

To understand these effects we need a detailed knowledge of defect processes whereby cerium is incorporated in the lattice. Such capability is provided by the computer simulation studies reported in this communication.

The atomistic simulation techniques used in this study have been widely used for metal oxide systems and are described extensively in the literature. The ionic model for solids is employed, where the total energy is partitioned into a short range contribution describing the repulsion and van der Waals attractions between electron charge clouds and long range Coulombic interactions. Parameters to describe the total energy as a function of nuclear co-ordinates are referred to as interatomic potentials, the quality of which are assessed by their ability to reproduce the observed crystal properties. The interatomic potentials[8–10] employed for the calculations detailed here have been used extensively for the study of many aspects of lanthanum perovskites by Islam *et al.*[4,8,11]

This investigation is concerned with charged defects; therefore, two particular aspects of the methodology are highlighted: the polarisable shell model and the Mott–Littleton formalism for treating the relaxation around a defect site. Charged defects polarise other ions in the lattice and therefore we require a treatment of ionic polarisability to be incorporated in the interatomic potential. The shell model of Dick and Overhauser[12] has been shown to simulate correctly dielectric and lattice dynamical properties of a wide variety of materials. The Mott–Littleton method of treating the relaxation around the defect site partitions the crystal into three regions, with the ions in the spherical inner region being allowed to relax to zero force, while the ions of region two are treated using the harmonic approximation, beyond which the outer ions are simulated by a quasi continuum method to infinity, as the effect of the defect is weak. The GULP code incorporates both lattice and defect models and has been used for all calculations reported.[13] In all calculations the radius of region one of the Mott–Littleton model was fixed at 10 Å, while the radius of region two was 20 Å.

Three mechanisms† have been considered for cerium doping: the first two are for doping stoichiometric $LaCoO_3$,

$$4La_{La}^{x} + 3CeO_2 \rightarrow 3Ce_{La}^{\bullet} + V_{La}^{\prime\prime\prime} + 2La_2O_3 \quad (1)$$

$$4La_{La}^{x} + 4CeO_2 + 4Co_{Co}^{x} \rightarrow 4Ce_{La}^{\bullet} + 4h_{Co}^{\prime} + 2La_2O_3 + O_2 \quad (2‡)$$

However, as prepared $LaCoO_3$ calcined at ≥ 900 °C is typically slightly reductively non-stoichiometric.[1] We have therefore considered the case of doping cerium into the $LaCoO_3$ lattice containing oxygen lattice vacancies according to eqn. (3).

$$2La_{La}^{x} + 2CeO_2 + V_O^{\bullet\bullet} \rightarrow 2Ce_{La}^{\bullet} + La_2O_3 + O_O^{x} \quad (3)$$

From the calculated energies collected in Table 1 we have calculated solution energies for each mechanism describing cerium insertion, shown in Table 2. From the solution energies for the first two mechanisms it is clear that Ce^{4+} is not soluble in stoichiometric $LaCoO_3$; however, the low solution energy for

Table 1 Lattice and defect energies for oxides

Static lattice energy/eV		Mott–Littleton defect energy/eV	
$LaCoO_3$	−143.07	La^{3+} vac	42.83
CeO_2	−105.64	Co^{2+} hole	31.04
La_2O_3	−127.35	O^{2-} vac	19.23
		Ce^{4+} sub	−32.12

DOI: 10.1039/b208392m

 This journal is © The Royal Society of Chemistry 2002

Table 2 Calculated solution energies/eV

E_{soln} [1]	2.89
E_{soln} [2]	2.7
E_{soln} [3]	0.23

the third mechanism shows that if cerium is inserted into the oxygen deficient lattice of $LaCoO_{3-\lambda}$ then there is much greater solubility. The non-stoichiometry of oxygen in the prepared catalysts is very difficult to characterise experimentally. For pure phase $LaCoO_3$ levels of oxygen have been found to be between 2.94 and 3.[15] Thus, the amount of cerium incorporation into the lattice can be considered to be dependent on the potential for this level of reductive non-stoichiometry (lack of oxygen) after undergoing typical high temperature preparation conditions for this material.

We have not considered doping of Ce^{4+} for Co^{3+} or Co^{2+} (the balancing defect for reductive non-stoichiometry) at the B site, as the ionic radius differ considerably. Ce^{4+} in an octahedral environment has an ionic radii of 0.87 whilst Co^{2+} and Co^{3+} in an octahedral environment have ionic radii of 0.65 and 0.61 respectively.[16] The V_{Co}''' and V_{Co}'' species are not reported as the $[CoO_6]$ unit is very stable in comparison to V_{La}''' formation.

It is interesting to compare the solubility of cerium, a tetravalent dopant, with Sr^{2+}, shown to be the most soluble divalent cation by Cherry *et al.*[8] The first two mechanisms have a much higher energy of solution than the values for Sr^{2+} doping, of 1.18 eV for $LaCoO_3$. However, the third mechanism shows that cerium will easily enter the lattice if oxygen vacancies are present, as it has a much lower solution energy than Sr^{2+}. The ionic radius for twelve fold coordinated ions can be compared, where Sr^{2+} is 1.44, which is slightly larger than that of La^{3+}, 1.36, whilst that of Ce^{4+}, 1.14, is much smaller.[16]

As mentioned earlier, the levels of oxygen vacancies present in single phase $LaCoO_3$ are up to 2%. The levels of cerium found in $La_{1-x}Ce_xCoO_{3-\lambda}$, before phase separation is observed, has been estimated as 1–4%.[17] Since one lattice oxygen vacancy is compensated by two dopant ions we can conclude that the calculated solution energy, by the third mechanism above, involving filling oxygen vacancies, is the only feasible mechanism for introducing a limited amount of Ce^{4+} into the lattice. *Once the oxygen vacancies are filled no more cerium can enter the lattice.*

For divalent Sr^{2+} doping, the importance of creating oxygen vacancies is again significant. As the A lattice site is reduced by substitution of a divalent cation there is a compensatory loss of oxygen from the lattice as the lowest energy mechanism.[4] The creation of oxygen vacancies leads to an increase in surface and sub-surface sites for oxygen adsorption and increased oxygen mobility at high temperature.[3,18–20] In contrast the effect of incorporating a tetravalent cation, using the third mechanism, is to oxidise the A site and therefore oxygen sites must be filled to charge compensate the lattice. Therefore, there will be a reduction in the number of vacancy sites for oxygen adsorption leading to a decrease in catalytic activity for lower temperature oxidation.[5]

Cerium does not improve the low temperature catalysis, before the onset of phase separation at $x > 0.05$. The low concentration of cerium in the lattice suggests that it does not perform the function of an active site for low temperature catalysis, but it has been speculated that it could stabilise surface Co^{3+}/O_2^- species under these conditions.[6] However, for the high temperature regime when the ion redox process $\frac{1}{2}\ O_2 + 2Co^{2+} + V_O^{\cdot\cdot} \Leftrightarrow 2Co^{3+} + O_O^x$, dominates,[2,3] catalyst performance becomes a complex function of factors governing the total availability of lattice oxygen for oxidation. The amount of oxygen at the surface and the sub-surface for release during oxidation and the rate of lattice replenishment is increased by the presence of some Ce^{4+} in the lattice, as shown by the low solution energy for the third mechanism proposed above, therefore leading to an improvement in catalyst performance.

We have performed calculations that demonstrate that cerium will only enter an oxygen deficient lattice, which we have postulated affects lower temperature suprafacial catalysis by reducing the number of oxygen vacancies for adsorption. However, at high temperatures the cerium pulls oxygen from the atmosphere into the lattice, filling vacancies and therefore providing additional oxygen for intrafacial catalysis.

SAF would like to thank ICI/Synetix for financial support, while M. S. Islam, A. A. Sokol, K. Wright and F. Cora are thanked for their useful insights.

Notes and references

† The Kröger–Vink defect notation is used, where a vacancy at the perovskite A site is denoted by V_A and a dopant species M at site A is given by M_A, while h_B describes the formation of a hole at the perovskite B site. The effective charge of the defect is shown by a superscript as positive $^\bullet$, negative $'$ or neutral ^{x}.

‡ O_2 is calculated using the method of Catlow.[14]

1 R. J. H. Voorhoeve, *Advanced Materials in Catalysis*, ed. J. J. Burton and R. L. Garten, Academic Press, New York, 1977, 129.
2 H. Arai, T. Yamada, K. Eguchi and T. Seiyama, *Appl. Catal.*, 1986, **26**, 265.
3 P. D. Petrolekas and I. S. Metcalfe, *J. Catal.*, 1995, **152**, 147.
4 M. S. D. Read, M. S. Islam, G. W. Watson, F. King and F. E. Hancock, *J. Mater. Chem.*, 2000, **10**, 2298.
5 C. Oliva, L. Forni, A. D'Ambrosio, F. Navarrini, A. D. Stepanov, Z. D. Kagramanov and A. I. Mikhailichenko, *Appl. Catal., A*, 2001, **205**, 245.
6 L. Forni, C. Oliva, F. P. Vatti, M. A. Kandala, A. M. Ezerets and A. V. Vishniakov, *Appl. Catal., B*, 1996, **7**, 269.
7 J. Kirchnerova, M. Alifanti and B. Delmon, *Appl. Catal., A*, 2002, **231**, 65.
8 M. Cherry, M. S. Islam and C. R. A. Catlow, *J. Solid State Chem.*, 1995, **118**, 125.
9 G. V. Lewis and C. R. A. Catlow, *J. Phys. C: Solid State Phys.*, 1985, **18**, 1149.
10 G. Balducci, M. S. Islam, J. Kapar, P. Fornasiero and M. Graziani, *Chem. Mater.*, 2000, **12**, 677.
11 M. S. Islam, *J. Mater. Chem.*, 2000, **10**, 1027.
12 B. G. Dick and A. Overhauser, *Phys. Rev.*, 1958, **112**, 90.
13 J. D. Gale, *J. Chem. Soc., Faraday Trans.*, 1997, **93**, 629.
14 C. R. A. Catlow, *J. Phys. Chem. Solids*, 1977, **38**, 1131.
15 M. O'Connell, A. K. Norman, C. F. Huttermann and M. A. Morris, *Catal. Today*, 1999, **47**, 123.
16 R. D. Shannon, *Acta. Crystallogr., Sect. A*, 1976, **32**, 751.
17 T. Nitadori and M. Misono, *J. Catal.*, 1985, **93**, 459.
18 D. Ferri and L. Forni, *Appl. Catal., B*, 1998, **16**, 119.
19 J. F. Howlett, W. R. Flavell, A. G. Thomas, J. Hollingworth, S. Warren, Z. Hashim, M. Mian, S. Squire, H. R. Aghabozorg, M. M. Sarker, P. L. Wincott, D. Teehan, S. Downes, D. S. L. Law and F. E. Hancock, *Faraday Discuss.*, 1996, 337.
20 L. G. Tejuca, J. L. G. Fierro and J. M. D. Tascon, *Adv. Catal.*, 1989, **36**, 237.

a new CONCISE INORGANIC CHEMISTRY

third edition

by

J. D. LEE

Senior Lecturer in Inorganic Chemistry
Loughborough University of Technology

Van Nostrand Reinhold (UK) Co. Ltd.

© J. D. Lee. 1964. 1965. 1977

First published 1964
Second edition 1965
Third edition 1977
Reprinted 1977, 1978, 1979, 1982

All rights reserved. No part of this work covered by the copyright hereon may be reproduced or used in any form or by any means – graphic, electronic, or mechanical, including photocopying, recording, taping, or information storage or retrieval systems – without written permission of the publishers

**Published by Van Nostrand Reinhold (UK) Co. Ltd.
Molly Millars Lane, Wokingham, Berkshire, England**

Library of Congress Cataloging in Publication Data

Lee, John David.
A new concise inorganic chemistry.

Editions for 1964 and 1965 published under title: Concise inorganic chemistry.
Bibliography: p.
Includes index.
1. Chemistry, Physical and theoretical.
2. Chemical bonds. I. Title. II. Title: Concise inorganic chemistry.
QD453.2.L43 1977 546 76–57657
ISBN 0–442–30169–3
ISBN 0–442–30165–0 pbk.
ISBN 0–442–30179–0 ELBS

Printed in Great Britain by Unwin Brothers of Woking

PREFACE

The aim of the first edition of this book was to provide a concise modern textbook of inorganic chemistry which was long enough to cover the essentials, yet short enough to be interesting. It provided a simple and logical theoretical framework into which the reader should be able to fit his factual knowledge. It was intended for those reading for Part I of the Grad.R.I.C. examinations, for first and second year students at universities and polytechnics, and for Higher National Certificate students at technical colleges. The aim of the third edition is still the same, and the layout of the book remains largely unchanged.

In the eleven years since the second edition of this book, chemical knowledge and understanding have advanced significantly. The molecular orbital theory of bonding has gained in popularity, and its coverage is extended, though the valence bond theory and electron pair repulsion (Sidgwick-Powell) concepts of bonding are still used extensively. The controversy over the extent to which *d* orbitals participate in σ bonding remains unresolved, and for simple compounds of the main groups the Gillespie-Nyholm concept of *d* orbitals participating in hybridization is retained.

About two thirds of the elements are metals, yet many chemistry books omit or give scant coverage to a discussion of bonding in metals and alloys. A new section has been included to rectify this.

Though there is a trend for chemistry teaching to become more theoretical most students eventually earn their living in an industrial environment, so an attempt has been made to indicate which chemicals are produced commercially on a large scale. Tonnage production figures inevitably vary from year to year, but still indicate the general scale of use.

There has been considerable interest in organometallic compounds, some of which are manufactured on a large scale (silicones, lead tetraethyl, Ziegler-Natta catalysts, etc.). These and the use of organolithium and Grignard reagents in syntheses are described in the appropriate groups. There has also been great interest in the role of inorganic materials in biological systems (chlorophyll, haemoglobin, vitamin B_{12} and nitrogen fixation) and a public awareness of the toxicity of various materials, most notably lead and mercury. These are discussed in the appropriate sections.

An enormous amount of effort has gone into the preparation and characterization of transition metal compounds and complexes, particularly using magnetic properties and visible and uv spectra. The discovery that a significant number of compounds of Cr, Mo, Tc, Re, Ru and Rh contain metal-metal bonds, and the discovery of metal atom cluster compounds for Nb, Ta, Mo, W

CHAPTER 7

f-BLOCK ELEMENTS

The Lanthanide Series (Table 7.1)

These 14 elements are alternatively called lanthanons, lanthanides or rare earths and are characterized by the filling up of the antepenultimate $4f$ energy levels.

TABLE 7.1

Element		Electronic structure		Oxidation states*		
		Xenon core				
Cerium	Ce	$4f^1\ 5d^1\ 6s^2$	$4f^2\ 6s^2$		+III	+IV
Praseodymium	Pr	$4f^2\ 5d^1\ 6s^2$	$4f^3\ 6s^2$		+III	(+IV)
Neodymium	Nd	$4f^3\ 5d^1\ 6s^2$	$4f^4\ 6s^2$	(+II?)	+III	(+IV?)
Promethium	Pm	$4f^4\ 5d^1\ 6s^2$	$4f^5\ 6s^2$		+III	
Samarium	Sm	$4f^5\ 5d^1\ 6s^2$	$4f^6\ 6s^2$	(+II)	+III	
Europium	Eu	$4f^6\ 5d^1\ 6s^2$	$4f^7\ 6s^2$	+II	+III	
Gadolinium	Gd	$4f^7\ 5d^1\ 6s^2$	$4f^7\ 5d^1\ 6s^2$	(+II?)	+III	
Terbium	Tb	$4f^8\ 5d^1\ 6s^2$	$4f^9\ 6s^2$		+III	(+IV)
Dysprosium	Dy	$4f^9\ 5d^1\ 6s^2$	$4f^{10}\ 6s^2$		+III	(+IV?)
Holmium	Ho	$4f^{10}\ 5d^1\ 6s^2$	$4f^{11}\ 6s^2$		+III	
Erbium	Er	$4f^{11}\ 5d^1\ 6s^2$	$4f^{12}\ 6s^2$		+III	
Thulium	Tm	$4f^{12}\ 5d^1\ 6s^2$	$4f^{13}\ 6s^2$	(+II?)	+III	
Ytterbium	Yb	$4f^{13}\ 5d^1\ 6s^2$	$4f^{14}\ 6s^2$	+II	+III	
Lutetium	Lu	$4f^{14}\ 5d^1\ 6s^2$	$4f^{14}\ 5d^1\ 6s^2$		+III	

*See p. 154.

Electronic Structure

The electronic structures of the lanthanide metals are not known for certain. Since lanthanum, the element preceding this series, has the electronic structure: xenon core $5d^16s^2$, it may be assumed that fourteen f electrons are filled in

from cerium to lutetium. By utilizing the two s electrons and the one d electron, trivalent metal ions might be expected. The lanthanides are characterized by the uniform (+III) oxidation state shown by all the metals.

An alternative electronic structure involves moving the single $5d$ electron into the $4f$ shell, except where this destroys the symmetry of a half full f shell. Which of the two arrangements is true is of little importance because the lanthanides typically form compounds which are ionic and trivalent, and the electronic structures of the ions are $Ce^{3+}f^1$, $Pr^{3+}f^2$, $Nd^{3+}f^3$, $Pm^{3+}f^4$, $Sm^{3+}f^5$....

The $4f$ electrons in the antepenultimate shell are very effectively screened from effects at the outside of the atom by the $5s$ and $5p$ electrons. Consequently the $4f$ electrons are not involved in the normal chemistry of these elements nor do they take part in bonding. This is in marked contrast to the considerable effect of filled or unfilled d levels on the sterochemistry and stability of transition metal compounds and complexes. Whether the f orbitals are filled or unfilled has little chemical effect, though it does affect their spectra and magnetic properties.

Oxidation States

The sum of the first three ionization energies are given in Table 7.2. The values are low, hence the elements are ionic and M^{3+} dominates the chemistry of these elements. The M^{2+} and M^{4+} ions that do occur are always less stable than M^{3+}. The most stable M^{2+} and M^{4+} ions are those which attain an f^0, f^7

TABLE 7.2

		$E°$ volts	Sum of first three ionization energies kJ mol^{-1}
Lanthanum	La	−2·52	3493
Cerium	Ce	−2·48	3512
Praseodymium	Pr	−2·47	3623
Neodymium	Nd	−2·44	3705
Promethium	Pm	−2·42	—
Samarium	Sm	−2·41	3898
Europium	Eu	−2·41	4033
Gadolinium	Gd	−2·40	3744
Terbium	Tb	−2·39	3792
Dysprosium	Dy	−2·35	3898
Holmium	Ho	−2·32	3937
Erbium	Er	−2·30	3908
Thulium	Tm	−2·28	4038
Ytterbium	Yb	−2·27	4197
Lutetium	Lu	−2·25	3898

or f^{14} configuration corresponding to an empty, half-full, or completely full f level (Ce^{4+} f shell empty, Eu^{2+} and Tb^{4+} f shell half full and Yb^{2+} f shell full). However, since Sm^{2+} and Tm^{2+} occur with f^6 and f^{13} arrangements and Pr^{4+} and Nd^{4+} have f^1 and f^2 arrangements there may be other factors. The (+II) and (+IV) states are not common, and are unstable in aqueous solution except for the well known Ce^{4+} salts such as ceric sulphate, which is used as an oxidizing agent in volumetric analyses.

Chemical Properties of (+III) Compounds

The chemical properties of the group are essentially the properties of trivalent ionic compounds. The metals are silvery white, and are electropositive and very reactive. They react slowly with cold water, and rapidly on heating.

$$M + H_2O \rightarrow M(OH)_3 + H_2$$

Their standard reduction potentials (E^0) are all high (Table 7.2). The hydroxides $M(OH)_3$ are precipitated from aqueous solutions by NH_4OH as gelatinous precipitates, which are ionic and basic. They are less basic than $Ca(OH)_2$ but more basic than the amphoteric $Al(OH)_3$. Thus they absorb CO_2 from the air and form carbonates. The basicity decreases as the ionic radius decreases from Ce → Lu. $Ce(OH)_3$ is the most basic, and $Lu(OH)_3$, which is the least basic, is intermediate between scandium and yttrium in basic strength.

The metals tarnish readily in air, and on heating in oxygen they all give oxides M_2O_3 except for Ce which forms CeO_2, and Y which forms a protective oxide film up to 1000 °C. The oxides are ionic and basic, and again basic strength decreases as the ions get smaller.

The metals reacts with H_2, but often require heating up to 300–400 °C to start the reaction. The products are nonstoichiometric compounds $\overline{MH}_2$ and $\overline{MH}_3$, which are remarkably stable to heat, often up to 900 °C. Their properties are intermediate between the ionic hydrides formed by the s block elements and the interstitial hydrides formed by the d block. They are decomposed by water, and react with oxygen.

$$\overline{CeH}_3 + H_2O \rightarrow Ce(OH)_3 + H_2$$

The anhydrous halides MX_3 can be made by heating the metal and halogen, or by heating the oxide with the appropriate ammonium halide.

$$M_2O_3 + 6NH_4Cl \xrightarrow{300\,^\circ C} 2MCl_3 + 6NH_3 + 3H_2O$$

The fluorides can be precipitated from solutions of M^{3+} by addition of F^- or HF. The fluorides are very insoluble, and this is used as a test for the lanthanides in qualitative analysis. However with excess F^-, the smaller lanthanide ions tend to form soluble $[MF^{2+}(aq)]$ complexes. The chlorides are deliquescent and soluble, and crystallize with six or seven molecules of water of crystallization. If these are heated, they form oxyhalides rather than dehydrate to anhydrous halides except for Ce which forms CeO_2.

$$MCl_3.6H_2O \xrightarrow{\text{heat}} MOCl + 5H_2O + 2HCl$$

The bromides and iodides are similar to the chlorides.

At elevated temperatures, the lanthanides react with B giving MB_4 and MB_6, with C giving MC_2 and M_2C_3, and with N, P, As, Sb and Bi giving MN etc.

A wide variety of oxysalts are known, including nitrates, carbonates, oxalates, sulphates, phosphates and strongly oxidizing ions such as perchlorates.

Oxidation States (+IV) and (+II)

The only (+IV) lanthanide which exists in solution is Ce^{4+}. The high charge on the ion leads to it being heavily hydrated, and except in strongly acid solutions the hydrated ion hydrolyses and gives polymeric species and H^+. Ce(IV) solutions are widely used as oxidizing agents, both in volumetric analysis and in organic reactions such as the oxidation of alcohols, aldehydes and ketones at the α carbon atom. The common compounds are CeO_2 (white when pure), $CeO_2.(H_2O)_n$ (a yellow gelatinous precipitate), CeF_4, ceric sulphate $Ce(SO_4)_2$ (yellow) and ceric ammonium nitrate. This was formerly represented $Ce(NO_3)_4.2(NH_4NO_3)$ but is now known to be $(NH_4)_2[Ce(NO_3)_6]$ with bidentate NO_3^- groups in the crystal structure and also in solution. CeO_2 is obtained by heating the metal in air, or heating $Ce_2^{III}(oxalate)_3$ in air. The oxide is insoluble in acids and alkalis, but dissolves if reduced giving Ce^{3+} solutions.

The most stable divalent lanthanide is Eu(II). $Eu^{II}SO_4$ can be prepared by electrolysing $Eu_2^{III}(SO_4)_3$ solutions, when the divalent sulphate is precipitated. $Eu^{II}Cl_2$ can be made as a solid by reducing $Eu^{III}Cl_3$ with H_2.

$$2EuCl_3 + H_2 \rightarrow 2EuCl_2 + 2HCl$$

Eu^{3+} solutions can be reduced by Na, Mg, Zn or zinc amalgam to give Eu^{2+}. EuH_2 is ionic and similar to CaH_2. In a number of ways Eu^{2+} resembles Ca^{2+}: the insolubility of the sulphate and carbonate, insolubility of the dichloride in strong HCl, solubility in liquid NH_3, but it differs in that the dihalides have a magnetic moment of 7·9 Bohr magnetons corresponding to seven unpaired electrons, and Eu^{2+} has a reduction potential of −0·41 volts, and is as strong a reducing agent as Cr^{2+}.

The elements Pr, Nd, Tb and Dy also form (+IV) states. These are generally unstable, occur only as solids, and are found as fluorides or oxides which may be nonstoichiometric.

S. Axen

Structure and Reactivity of Perovskite-Type Oxides

LUIS G. TEJUCA AND JOSÉ LUIS G. FIERRO

Instituto de Catálisis y Petroleoquímica
C.S.I.C.
Serrano 119, 28006 Madrid, Spain

AND

JUAN M. D. TASCÓN

Instituto Nacional del Carbón y sus Derivados
C.S.I.C.
Apartado 73, 33080 Oviedo, Spain

I. Introduction

Perovskite-type oxides have the general formula ABO_3 (A, cation of larger size) and are structurally similar to $CaTiO_3$, the mineral that gave its name to that group of compounds. These materials were first studied because of their important physical properties such as ferro-, piezo-, and pyroelectricity, magnetism and electrooptic effects. The earliest works where perovskites were used as catalysts were conducted in 1952 and 1953 by Parravano (*1*, *2*), who observed that the rate of the catalytic oxidation of carbon monoxide is affected by ferroelectric transitions in $NaNbO_3$, $KNbO_3$, and $LaFeO_3$ (*1*). This may be interpreted as evidence supporting an electronic mechanism for this reaction. A similar effect in the rate of CO oxidation was observed in the neighborhood of the ferromagnetic transition in $La_{0.65}Sr_{0.35}MnO_3$ (*2*). Years later, Dickens and Whittingham (*3*) reported data on the recombination of oxygen atoms on the surface of alkali metal tungsten bronzes M_xWO_3, where M = Li, Na, or K. The catalytic activities were found to be closely related to the electronic properties of the bronzes. Galasso (*4*) reported a study carried out by Epperly *et al.* (*5*) on the application of $A(BB')O_3$ oxides as electrodes for fuel cells; B and B′ cations were selected, respectively, for

Copyright © 1989 by Academic Press, Inc.
All rights of reproduction in any form reserved.

genation, and dehydration of 2-propanol. Potential applications for coal liquefaction and removal of carbonaceous deposits from coked catalysts are also considered. Section VII,J refers to SO_2 adsorption on A, B, and oxygen sites and its effect in the catalytic performance of perovskites for CO and hydrocarbon oxidation. Section VIII describes other applications of perovskites such as in actinide storage in radioactive waste, in solid-state chemical sensors and in superconductivity at high temperatures. Finally, in Section IX some prospective lines of research are suggested.

II. Structure

A. The Perovskite Structure

The ideal perovskite-type structure is cubic, with space group $Pm3m$-O_h^1. Its unit formula is ABX_3, where A is the larger cation, B is the smaller cation, and X is an anion. In this structure, the B cation is in a six-fold coordination and the A cation is in a twelvefold coordination with the anions. Figure 2a shows the corner-sharing octahedral units that form the skeleton of the structure (stabilized by the Madelung energy), whose body-center position is occupied by the A cation. Alternatively, the structure can be viewed with the B cation in the center, as shown in Fig. 2b. The perovskite structure is thus a superstructure with a ReO_3-type framework, formed by the introduction of A cations into the BX_3 octahedra building. Raveau (*18*) has recently pointed out the important role of the ReO_3 framework as a host structure for deriving numerous structures of complex oxides.

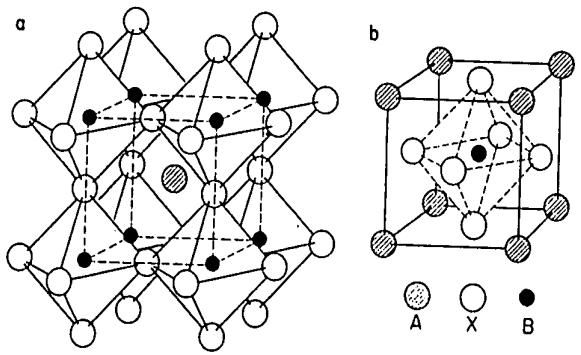

FIG. 2. ABX_3 ideal perovskite structure: (a), cation A, or (b), cation B, at the center of the unit cell. (Reprinted by permission from Ref. *15*.)

The lower limits for cationic radii are $r_A > 0.09$ nm, and $r_B > 0.051$ nm in the case of oxides. Goldschmidt (*19*), on the basis of geometric considerations, defined the tolerance limits of the size of ions through a tolerance factor $t = (r_A + r_X)/\sqrt{2}(r_B + r_X)$, where r_A, r_B, and r_X are the radii of the respective ions; t would be equal to one for the ideal cubic structure (Fig. 2). In fact, the perovskite structure exists in oxides only between the limits $0.75 < t < 1.0$ with t between 0.8 and 0.9 in most cases. For $t > 1$ the calcite and aragonite structures are prevalent, whereas for $t < 0.75$ the stable structure is ilmenite. Roth (*20*) has classified the limits of the existence of these competing structures according to the ionic radii values.

Besides the ionic radii requirements, the other condition to be fulfilled is electroneutrality, i.e., that the sum of charges of A and B ions equals the total charge of X anions. This is attained in the case of oxides by means of charge distribution of the form $A^{1+}B^{5+}O_3$, $A^{2+}B^{4+}O_3$, or $A^{3+}B^{3+}O_3$. Moreover, partial substitution of A and B ions giving rise to complex oxides is possible while keeping the perovskite structure. Figure 3, elaborated from some comprehensive compilations of data on the structure and properties of this type of compound (*4*, *15*, *17*, *21*, *22*), shows that almost all the stable elements have been included in the perovskite framework, many of them in both the A and B positions. In what follows we will

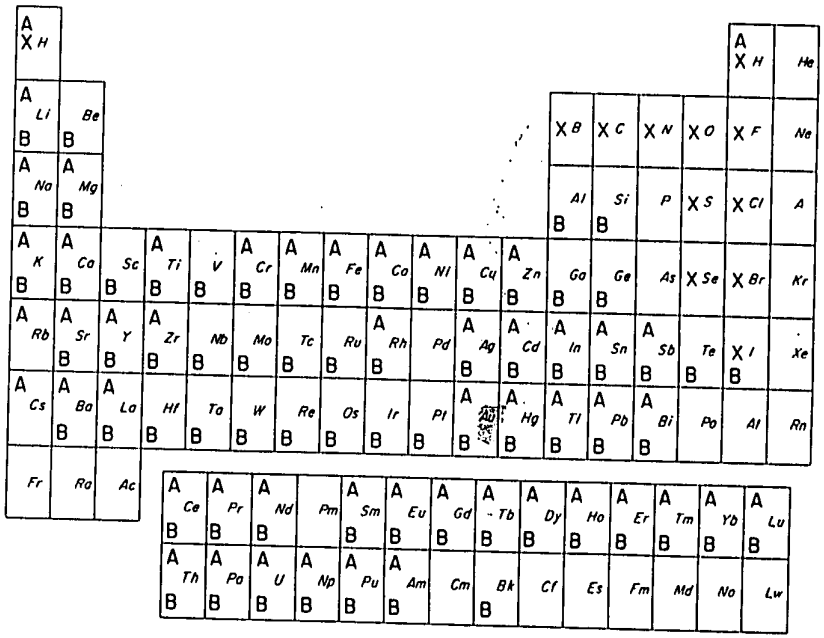

FIG. 3. Survey of the chemical elements that are known to be stable in the A, B, and/or X positions of the perovskite structure.

limit the structural description of perovskites to the case of X = oxygen, for the reasons indicated in Section VII,I.

The ideal perovskite structure appears only in a few cases for tolerance factors very close to 1 and at high temperatures. In other conditions different distortions of the perovskite structure will appear. The compound $CaTiO_3$ was originally thought to be cubic, but the true symmetry was later shown to be orthorhombic (*23*). Distorted structures with orthorhombic, rhombohedral, tetragonal, monoclinic, and triclinic symmetries are known, but the last three types are very rare and poorly characterized (*21*), so we will only describe the orthorhombic and rhombohedral distortions.

For t values in the range of $0.75 < t < 0.90$ a cooperative buckling of corner-shared octahedra takes place, leading to the orthorhombic distortion. This network, sometimes typified as $GdFeO_3$ structure, has a space group *Pbnm*, and its relationship to the perovskite structure is as shown in Fig. 4a. It is obtained by tilting oxygen octahedra in such a way that the A atoms are displaced along (1, $\bar{1}$, 0) pseudocubic directions or (0, 1, 0) directions. The true orthorhombic cell is usually referred to as "*O*-orthorhombic," characterized by a lattice parameter ratio $(c/a) > \sqrt{2}$, to be distinguished from the *O'*-orthorhombic structure, with $(c/a) < \sqrt{2}$. This latter form is the result of a superimposed Jahn–Teller distortion of the perovskite structure. When there is no octahedra buckling, a small deformation from cubic to rhombohedral symmetry may take place. This occurs for tolerance factors in the range of $0.9 < t < 1.0$. The rhombohedral distortion, sometimes referred to as "$LaAlO_3$ structure," has the $R\bar{3}c$-D_{3d}^6 symmetry. Its relationship to an ideal perovskite is shown in Fig. 4b. In most cases the anions are displaced, thus requiring a large unit cell; in the most general situation the anion displacements may be decomposed into $R\bar{3}c$ and $R\bar{3}m$ components.

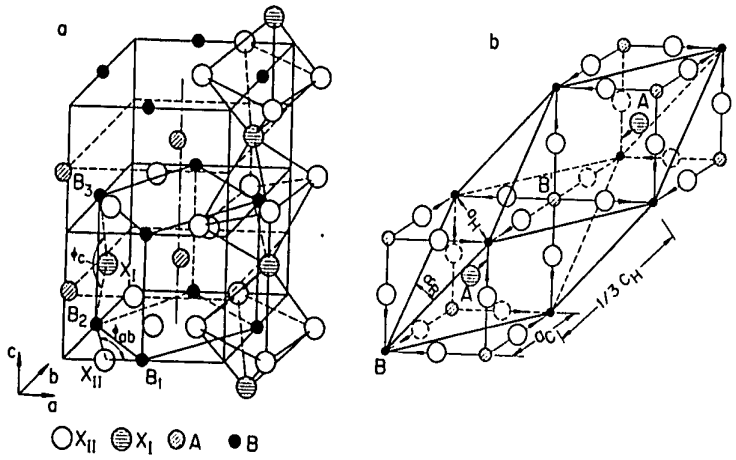

FIG. 4. Orthorhombic (a) and rhombohedral (b) distortions of the perovskite structure. (Reprinted by permission from Ref. *15*.)

Nonstoichiometry in perovskites can arise from either cation deficiency (in the A or B site), anion deficiency, or anion excess. This subject has been widely discussed in some excellent reviews (*24*, *25*); thus, we will focus only on general features of the different types of nonstoichiometry. Because of the stability of the BO_3 groups, A cations can be missing without collapse of the perovskite network. The ReO_3-type structure is thus the limiting case of A-site vacancy nonstoichiometry. The most typical example is that of tungsten bronzes, A_xWO_3. The question as to whether A-site atoms and vacancies are ordered is not fully resolved (*24*). Because of the large formal charge and the small size of the B cations in perovskites, B-site vacancies are not energetically favored; B–B interactions, which may be a compensating factor, are favored by hexagonal stacking of AO_3 layers. Accordingly, a number of hexagonal perovskites exhibiting B-site vacancies have been described (*24*). Normally, these vacancies are ordered between *h*–*h* layers where the BO_6 octahedra share faces, in agreement with Pauling's rules for the sharing of coordination polyhedra.

Anion vacancy in perovskites is more common than cation vacancy. Unlike the well-known case of WO_3, anion-deficient nonstoichiometry is not accommodated by the crystallographic shear mechanism, but by assimilation of vacancies into the structure, resulting in supercells of the basic network. The review by Rao *et al.* (*24*) contains numerous examples of this kind of behavior. Anion excess has been described in a more limited number of systems. Structural details of this type of compounds can be found in Rao *et al.* (*24*) and Smyth (*25*).

B. Related Structures

The strong bonding between B-site ions and oxygen ions leads to retention of the BO_3 grouping even when a three-dimensional network is no longer permitted by stoichiometry. The simplest case is that of the SnF_4-type structure, consisting of the superposition of octahedra nets, with the free peaks of octahedra of one layer lying in the holes formed between the peaks of octahedra in the neighboring layers. The peaks of octahedra are sunk so deeply into these holes that an almost planar structure is obtained. In the K_2NiF_4-type compounds, slices of the perovskite structure